Check for updates

CHEMISTRY
A European Journal

A Journal of
ChemPubSoc Europe

Accepted Article

Title: Fully sp²-Carbon-Linked Crystalline Two-Dimensional Conjugated Polymers: Insight into 2D Poly(Phenylenecyanovinylene) Formation and their Optoelectronic Properties

Authors: Daniel Becker, Bishnu Prasad Biswal, Paula Kaleńczuk, Naisa Chandrasekhar, Lars Giebeler, Matthew Addicoat, Silvia Paasch, Eike Brunner, Karl Leo, Arezoo Dianat, Gianaurelio Cuniberti, Reinhard Berger, and Xinliang Feng

This manuscript has been accepted after peer review and appears as an Accepted Article online prior to editing, proofing, and formal publication of the final Version of Record (VoR). This work is currently citable by using the Digital Object Identifier (DOI) given below. The VoR will be published online in Early View as soon as possible and may be different to this Accepted Article as a result of editing. Readers should obtain the VoR from the journal website shown below when it is published to ensure accuracy of information. The authors are responsible for the content of this Accepted Article.

To be cited as: *Chem. Eur. J.* 10.1002/chem.201806385

Link to VoR: http://dx.doi.org/10.1002/chem.201806385

Supported by
ACES

WILEY-VCH

10.1002/chem.201806385

WILEY-VCH

Fully sp^2-Carbon-Linked Crystalline Two-Dimensional Conjugated Polymers: Insight into 2D Poly(Phenylenecyanovinylene) Formation and Their Optoelectronic Properties

Daniel Becker,[a],‡ Bishnu P. Biswal,[a],‡ Paula Kaleńczuk,[a] Naisa Chandrasekhar,[a] Lars Giebeler,[b] Matthew Addicoat,[c] Silvia Paasch,[d] Eike Brunner,[d] Karl Leo,[e] Arezoo Dianat,[f] Gianaurelio Cuniberti,[f] Reinhard Berger,*[a] Xinliang Feng*[a]

Abstract: Cyano-substituted polyphenylene vinylenes (PPVs) have been in the focus of research for several decades due to their interesting optoelectronic properties and potential applications in organic electronics. With the advent of organic two-dimensional (2D) crystals, the question arose how the chemical and optoelectronic advantages of PPVs evolve in 2D compared to their linear counterparts. In this work, we present the efficent synthesis of two novel 2D fully sp²-carbon-linked crystalline PPVs and investigate the essentiality of inorganic bases for their catalytic formation. Notably, among all bases screened, cesium carbonate (Cs_2CO_3) plays a crucial role and enables reversibility in the first step with subsequent structure locking by formation of a C=C double bond to maintain crystallinity, which is supported by density functional theory (DFT) calculation. We propose a quantifiable energy diagram of a "quasi-reversible reaction" which allows to identify further suitable C-C bond formation reactions for 2D polymerizations. Moreover, we delineate the narrowing of the HOMO-LUMO gap by expanding conjugation into two dimensions. To enable environmentally benign processing, we further perform the post-modification of 2D PPVs, which renders stable dispersions in the aqueous phase.

Introduction

Since the discovery of electrical conductivity in polyacetylene through doping in 1977,[1] linear conjugated polymers are an important materials class for applications in organic light-emitting diodes, organic photovoltaics and organic field-effect transistors.[2] In contrast to linear conjugated polymers, extension of conjugation in two dimension (2D) has fascinated theoreticians for several decades.[3] However, it was only until the discovery of graphene in 2004 that 2D conjugated polymer frameworks become emerging synthetic targets for experimental chemists because graphene has demonstrated outstanding physical properties, including high room temperature mobility of $\mu = 2.5 \times 10^5$ cm^2 V^{-1} s^{-1}, Young modulus of 1 TPa and intrinsic strength of 130 GPa, e.g.[4] Conjugation in 2D directions can offer multiple conjugation pathways and thus can overcome the problem of limited conjugation lengths and possible point defects. On a fundamental level, extending the conjugation significantly alters the electronic structure of conjugated polymers compared to their linear cases. It has been theoretically predicted that the energy gap between highest occupied molecular orbital (HOMO) and lowest unoccupied molecular orbital (LUMO) evolves faster in the 2D structure, whereas the experimental proof is still missing.[5]

Towards the synthesis of 2D conjugated polymers, several strategies have been attempted so far. For instance, a *meta*-connected 2D polyphenylene as the "porous graphene" and covalent assemblies of porphyrin monomers have been reported via the on-surface synthesis under ultra-high vacuum conditions.[6] However, a transfer of such metal surface-binding 2D conjugated polymers is a difficult issue. Recently, a solid-state polymerization approach was presented, which nonetheless required the monomers pre-arranged in bulk crystals, thus limiting the kind of monomers and type of reactions.[7] 2D π-conjugated covalent organic frameworks (COFs), which are also considered as stacked, crystalline 2D conjugated polymers, are typically formed by employing reversible condensation reactions in solution synthesis approach. They mostly contain C=N linkages, which lack efficient conjugation.[8] In contrast, 2D conjugated polymer backbones consisting of entirely C=C linkages which would provide superior conjugation as well as chemical and electrochemical stabilities, remain an enormous synthetic challenge.[9,10] Despite of the recent progress in the synthesis of sp²-carbon-linked 2D conjugated polymers by Knoevenagel polycondensation reaction, the formation mechanism is still unknown which hampers the establishment of a robust synthetic methodology for the further development of related materials and applications.[11].

Herein, we demonstrate the efficient synthesis of two novel 2D cyano-substituted poly(phenylene vinylene)s (**CN-PPV**s), namely **2D-CN-PPV-1** and **-2** (Scheme 1a) by controlling the Knoevenagel polycondensation reaction between 1,3,5-tris(4-cyanomethylphenyl)benzene (**TCPB**) with 1,3,5-tris(4-formyl-

[a] D. Becker,‡ Dr. B. P. Biswal,‡ P. Kaleńczuk, Dr. N. Chandrasekhar, Dr. R. Berger, Prof. Dr. X. Feng
Faculty of Chemistry and Food Chemistry, Center for Advancing Electronics Dresden, Technische Universitat Dresden, 01062, Dresden, Germany.
E-mail: xinliang.feng@tu-dresden.de; reinhard.berger@tu-dresden.de
[b] Dr. L. Giebeler
Department Chemistry of Functional Materials, Leibniz Institute for Solid State and Materials Research Dresden, Helmholtzstr. 20, 01069 Dresden, Germany
[c] Dr. M. Addicoat
School of Science and Technology, Nottingham Trent University, Clifton Lane, Nottingham, NG11 8NS, UK
[d] Dr. S. Paasch, Prof. Dr. E. Brunner
Chair of Bioanalytical Chemistry, Technische Universität Dresden, 01069, Dresden, Germany.
[e] Prof. Dr. Karl Leo
Dresden Integrated Center for Applied Physics and Photonic Materials (IAPP), Nöthnitzer Str. 61, 01187 Dresden
[f] Dr. A. Dianat, Prof. Dr. G. Cuniberti
Institute for Materials Science, Technische Universität Dresden, 01062, Dresden, Germany.
[‡] These authors contributed equally to this work.
Supporting Information and the ORCID number(s) for the author(s) of this article can be found under https://doi.org/xxxxxxxxxxxxx.

This article is protected by copyright. All rights reserved.

Accepted Manuscript

phenyl)benzene (**TFPB**) and 4,4'-biphenyldicarboxaldehyde (**BPDA**), respectively.

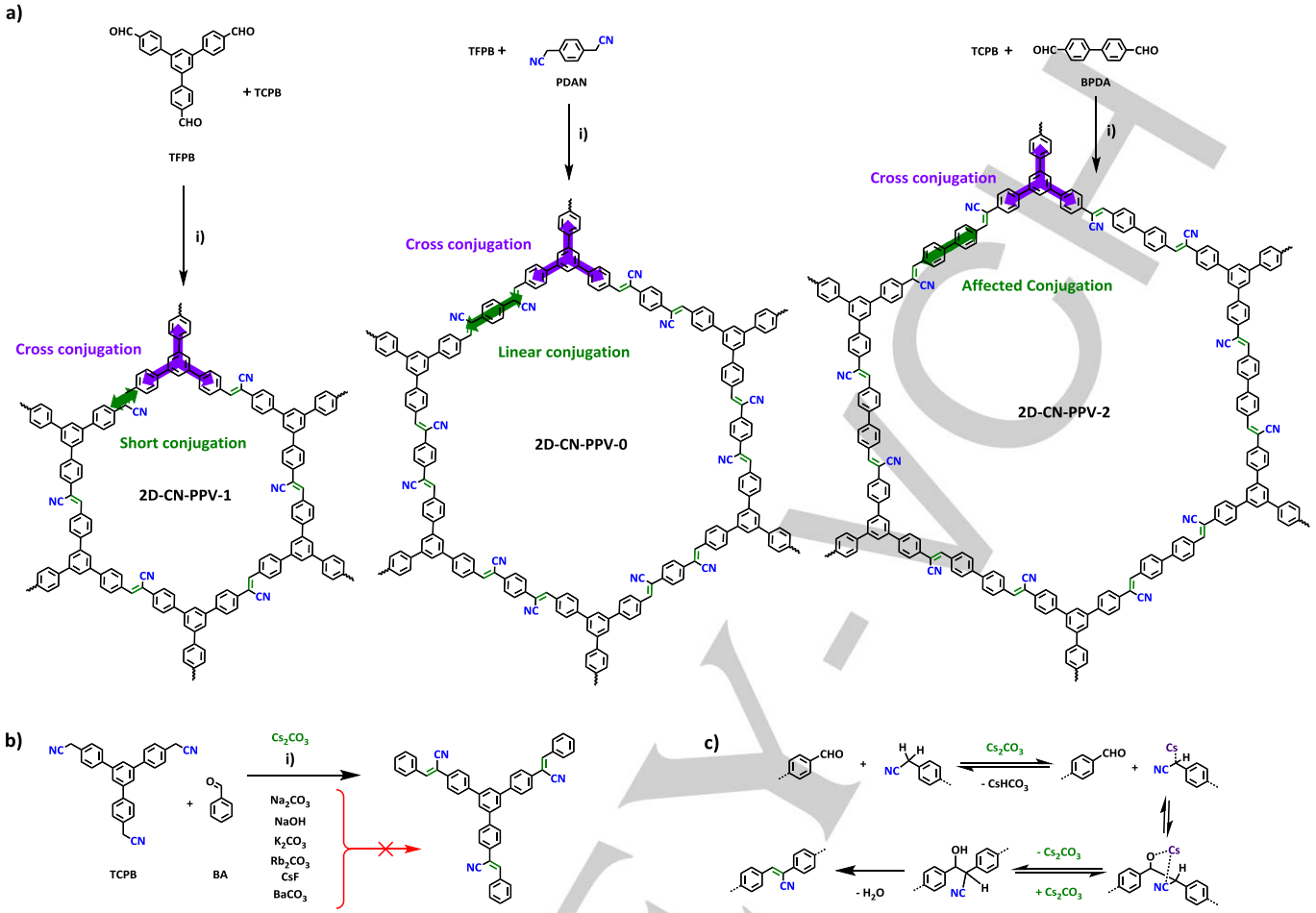

Scheme 1. Schematic illustration of Knoevenagel polycondensation reaction employed in a) formation of crystalline 2D-CN-PPVs and demonstration of the conjugation degree, i) Cs_2CO_3; *o*-DCB, 120 ºC, 3 days; b) model reactions resembling solvothermal conditions with inorganic Lewis bases optimization; c) Proposed Cs_2CO_3 mediated reaction pathway for the formation of 2D-CN-PPVs.

The chemical structure and long range ordering of the targeted **2D-CN-PPV**s have been unambiguously confirmed by Fourier transformed Infrared Spectroscopy (FT-IR), ^{13}C cross-polarization magic-angle spinning (CP-MAS) NMR and powder X-ray diffraction (P-XRD). In order to gain insight into the propagation mechanism of the polymerization step, we examined the essentiality of inorganic bases by means of DFT-NEB theoretical modelling. Importantly, we observed that Cs_2CO_3 inherits the unique ability to facilitate reversible C-C bond formation and lower activation energy in the first step in contrast to all other applied bases, which are crucial for the final crystalline 2D polymer formation. Furthermore, we explored the optoelectronic characterizations of these **2D PPV**s employing Ultraviolet/Visible (UV/Vis), photoluminescence (PL) spectroscopy and cyclic voltammetry (CV). Moreover, the evolution of band gaps by improved conjugation of three different **2D-CN-PPV**s was clearly demonstrated. Finally, a post-modification has been developed on **2D-CN-PPV**s to improve the dispersibility in aqueous phase for better solution processability, which can be essential for the application of such new polymeric materials for thin-film based devices.

Result and Discussion

The polymerizations toward targeted **2D-CN-PPV**s (Scheme 1a) were achieved by employing Knoevenagel condensation reactions of aromatic aldehydes such as **TFPB**, **BPDA** and **TCPB**, respectively. For comparison, we also synthesized the earlier reported polymer, namely **2D-CN-PPV-0**, starting from **TFPB** and 1,4-bis(cyanomethyl)benzene (phenylenediacetonitrile, **PDAN**).[9] In addition, we investigated the effect of polymerization efficiency by examining the homologous row of alkali metal carbonates (from Na to Cs), CsF, $BaCO_3$ and NaOH in model reactions resembling the solvothermal conditions (*o*-DCB, 120 °C, 3 days) between **TCPB** and benzaldehyde (Scheme 1b). It has been noticed that, from all applied Lewis bases, only Cs_2CO_3 (84% yield) and $BaCO_3$ (53%) yielded the model compound. In agreement, targeted crystalline 2D conjugated polymers resulted only from using Cs_2CO_3, while no other bases worked at all. This result strongly suggests that Cs_2CO_3 plays an important and particular role. To understand the role of Cs_2CO_3 in the Knoevenagel condensation reaction (Scheme 1c), we examined

This article is protected by copyright. All rights reserved.

Accepted Manuscript

the reaction mechanism by means of DFT – nudged elastic band (NEB) calculations by considering one condensation step between TFPB and TCPB (Figure 1). We observed that among all bases studied (see Figure S10-1, Electronic Supplementary Information), Cs_2CO_3 is able to reduce the energy barrier on the way towards the initial C-C single bond from stage 1 (STG1) to STG3 most effectively as shown in Figure 1. Through bridging oxygen and nitrogen, forming a five-membered transition state (Figure 1, STG3), Cs^+ can well stabilize the intermediate state.

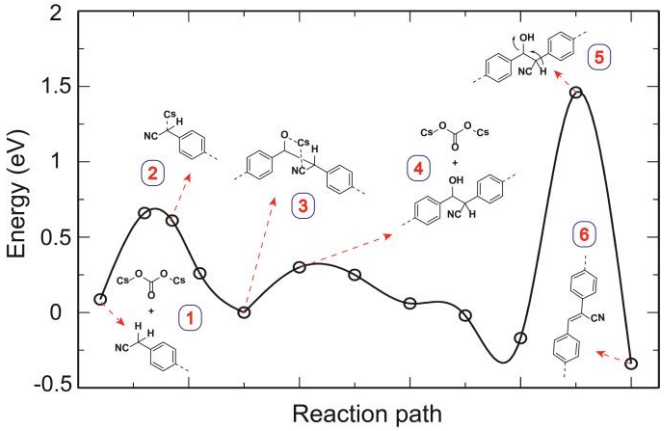

Figure 1. Energy profiles at different stages (STG1-6) calculated in eV using DFT-NEB method describing the proposed reaction mechanism.

However, its energy is slightly higher than the comparable intermediates employing Li^+ and Na^+ ions (see Figure S10-1, ESI). Therefore, the energetic position of STG3 seems to promote bond cleavage and thus the back reaction: On the one hand from intermediate STG3 C-C-bond cleavage back into STG2 is possible as well as on the other hand continuation of the reaction path via protonation of STG3 and the release of Cs_2CO_3 into STG4. After a subsequent elimination of water in STG5, the formation of the targeted C=C double bond in the final STG6 is possible. The energy barrier for the condensation step (Figure 1, STG5) can be overcome easily by thermal fluctuations with all alkali metal carbonates. Taken these results into account Cs_2CO_3 seems to play a specific role due to its size,[12] which has the ability to bridge oxygen and nitrogen, to stabilize the carbanion in STG2 and to slightly but importantly destabilize the intermediate STG3. As the result, it enables a polymer growth with a "quasi-reversible" C-C bond formation. Such error correcting process is assumed to play the key role in achieving crystalline 2D conjugated polymer structures. We propose, that DFT – NEB calculation allows to draw a quantifiable energy diagram of a "quasi-reversible" reaction and may identify suitable C-C bond formation reaction for 2D polymerization during or even before experimental "try and error" screening. The chemical composition and functional groups of all **2D-CN-PPV**s are confirmed by FT-IR and CP-MAS NMR characterizations. In the FT-IR spectra (Figure S3-1 – S3-4, ESI), the C=C stretch signal is identified at 3050 cm^{-1} for all **2D-CN-PPV**s. Further, the appearance of a peak at 2250 cm^{-1} from the nitrile groups and the negligible peak at 1667 cm^{-1} corresponding to the aldehyde group of the starting monomers suggest high polymerization efficiency. The CP-MAS NMR spectra of all the **2D-CN-PPV**s (Figure 2a) show a similar pattern with clear peak resolution, which refers to a high degree of structural ordering. The chemical shift of quaternary benzene ring-C atoms appears at 141 ppm along with the tertiary benzene C-atoms at 127 ppm. The chemical shift of the C-atom attached to the nitrile group is assigned to 132 ppm, the quaternary C-atom neighbouring the nitrile group at 110 ppm, and the nitrile-C at 119 ppm. No residual aldehyde peak was observed, which would be expected at 191 ppm compared with the CP-MAS NMR spectra of the monomer (Figure S3-6, ESI) which supports the polymerization efficiency. Thermogravimetric analyses (TGA) disclose that all three **2D-CN-PPV**s have excellent thermal stabilities up to 400°C (Figure S6-3, ESI).

Scanning electron microscopy (SEM) and transmission electron microscope (TEM) imaging were performed to unravel the morphology of these **2D-CN-PPV**s. Toward this end, **2D-CN-PPV**s were exfoliated by mechanical grinding for 15 min. and followed by sonication in ethanol. The as-prepared dispersions were filtered through a syringe filter and drop-casted on the substrate. In all cases they show layered morphologies with sizes up to 10 µm (Figure 2c-e and Figure S7-1, ESI). In order to prove the regioregular crystalline 2D structure in each **2D-CN-PPV**s, (P-XRD) measurements were conducted. The first intense reflection for **2D-CN-PPV-1** was observed at 3.91° 2θ corresponding to the (100) plane along with other minor reflections at 6.91°, 7.94° and 8.30° 2θ. Similarly for **2D-CN-PPV-0** and **2D-CN-PPV-2** the first reflection appeared at 2.74° and 2.27° 2θ, respectively, which are attributed to the (100) plane. **2D-CN-PPV-2** with the **BPDA** spacer only shows two major reflections in the P-XRD pattern, indicating moderate crystallinity (Figure 2b). This observation could be explained by the lower shape persistency of the starting monomers leading to weaker interlayer π-π stacking and therefore worse alignment in the plane.[13] The structures of all the **2D-CN-PPV**s were optimized in typical eclipsed (AA), staggered (AB) and slipped eclipsed (slip-AA) π-π stacking arrangements using the Density Functional Tight Binding method. It has been found that the experimental P-XRD of all **2D-CN-PPV**s are matched well with the simulated one derived from the eclipsed (AA) π-π stacking arrangement (Figure S4-1 – S4-3, ESI).

Further, the Pawley refinement was carried out for **2D-CN-PPV-1** and **-2** to calculate the lattice parameter using the same AA model (Figure S4-5 and S4-6, ESI). In their stacked form, the permanent porosity and pore size distribution of 2D-CN-PPV powders were determined through N_2 physisorption measurements at 77 K (Figure S6-1 and S6-2).[14] Reversible type I adsorption-desorption isotherms with specific surface areas of 301 $m^2\ g^{-1}$ for **2D-CN-PPV-1** and 638 $m^2\ g^{-1}$ for **2D-CN-PPV-2**, respectively, according to the Brunauer-Emmett-Teller model in the relative pressure range 0.01 to 0.2, were found. From the N_2 adsorption data the pore size distributions were calculated using the Non-Local Density Functional Theory (NLDFT) model, which shows the primary peak positioned at 1.45 nm for **2D-CN-PPV-1** and 3.24 nm for **2D-CN-PPV-2**, respectively. The experimentally determined pore sizes are slightly smaller than the predicted values from the structural models (2.1 nm for **2D-CN-PPV-1** and 4.0 nm for **2D-CN-PPV-2**), which are attributed to the eclipsed stacking arrangements.

To gain insight into the fundamental optoelectronic properties of the **2D-CN-PPV**s, we performed UV-Vis (Figure 3a) and photoluminescence (PL) spectroscopic experiments (Figure 3b). Measurements were carried out with as-prepared dispersions (~1 mg mL^{-1}) in isopropanol in the center of an Ulbricht sphere to avoid the contribution of reflectance.[15] **2D-CN-PPV-1** shows an absorption band centered at 368 nm, **2D-CN-PPV-0** at 372 nm and **2D-CN-PPV-2** at 384 nm with corresponding absorption edges of 460, 501 and 488 nm, respectively. These values correspond to optical band gaps of 2.70, 2.47 and 2.54 eV for **2D-CN-PPV-1**, **2D-CN-PPV-0** and **2D-CN-PPV-2**, respectively.[16] The visual appearance of all **2D-CN-PPV** dispersions under UV light exposure is shown in Figure 3d. For comparison, we carried out

Accepted Manuscript

This article is protected by copyright. All rights reserved.

the UV-Vis measurement in solid state and observed a good agreement with the absorption from dispersion with only a slight bathochromic shift of the maximum absorption for all three polymers in the range of 11 to 26 nm.[17] PL measurements were performed in dispersions in isopropanol (5 mg mL^{-1}). All **2D-CN-PPV** materials showed strong and distinct fluorescence at 498, 550 and 511 nm with PL quantum yields of 5%, 3.5% and 8.1% for **2D-CN-PPV-1, -0**, and **-2**, respectively.[18]

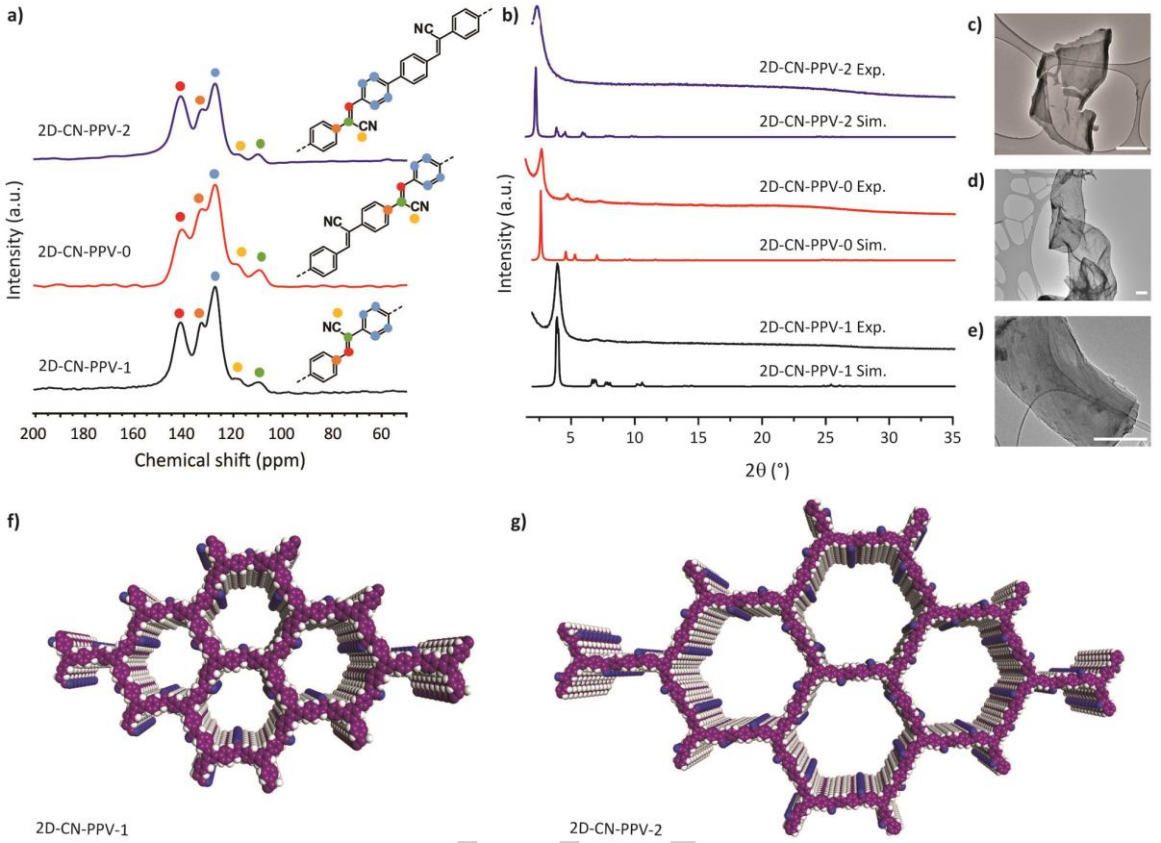

Figure 2. Evaluation of chemical structure, morphology and crystallinity of 2D-CN-PPVs. a) CP-MAS NMR spectra; b) experimental and simulated P-XRD patterns of 2D-CN-PPV-2 (blue), 2D-CN-PPV-0 (red) and 2D-CN-PPV-1 (black); c), d) and e) TEM images of mechanochemically exfoliated 2D-CN-PPV-2 , 2D-CN-PPV-0 and 2D-CN-PPV-1, respectively, after sonication in ethanol. Scale bar 500 nm. f) and g) show the spacefill models of the two new synthesized 2D-CN-PPV-1 and -2, respectively.

Additionally, cyclic voltammetry (CV, Figure 3c) was performed on the drop-casted samples of **2D-CN-PPV**s. In all systems, a quasi-reversible reduction step at -0.76, -0.85 and 0.78 V was observed, corresponding to LUMO values of -3.41, -3.44 and -3.42 eV and irreversible oxidation at 1.30, 1.21 and 1.26 eV for **2D-CN-PPV-1, -0**, and **-2**, respectively. All optoelectronic data are summarized and compared to the linear PPV counterparts (Table S9-1, ESI). Apparently, the band gap decreases from 2.70 eV for **2D-CN-PPV-1** to 2.47 eV for **2D-CN-PPV-0** by 0.23 eV. This behaviour is explained by the longer conjugation length of the linear linkage contribution (Scheme 1a). Although, for **2D-CN-PPV-2** lateral extension by one additional phenylene is introduced, the increase of the optical band gap is likely due to the higher twisting degree of biphenylene unit and, therefore, affected conjugation degree (see Scheme 1a). The same trend is found for the UV-Vis absorption maxima and is supported by theoretical modelling on the single layer 2D conjugated polymers. Interestingly, the optical band gaps of **2D-CN-PPV-0** and **2D-CN-PPV-2** are in the same range as the *para*-connected **1D-CN-PPV**. Only the band gap of **2D-CN-PPV-1** is slightly higher (2.7 eV). It should be emphasized that in the linear **1D-CN-PPV** only *para*-connection is employed, whereas, the percentage of strictly *para*-linkage in the **2D-CN-PPV**s is very limited. This result strongly suggests that the **2D-CN-PPV**s own significant cross-conjugation along the *meta*-direction. The experimental energy band gaps of reported linear *meta*-connected **CN-PPV** polymers are found to be at 2.7 eV and generally higher than the *para*-connected counterparts and herein the achieved **2D-CN-PPV**s.[17,18] With this series of **2D-CN-PPV**s in our hand, our results for the first time experimentally demonstrate the declining effect of the HOMO-LUMO gap for 2D conjugated polymers with increasing conjugation. As similar to many other 2D layered materials, one major drawback of 2D conjugated polymers can be their poor solution processability. Therefore, to increase the dispersibility and processability of **2D-CN-PPV**s from environmentally friendly solvents, we further hydrolysed **2D-CN-PPV-1** in basic conditions, which produced **2D-COOH-PPV-1** (Figure 4a, experimental procedure can be found in Supplementary Information). The carboxylic acid moieties of **2D-COOH-PPV-1** increase the water affinity and the water vapor uptake in comparison to the parent **2D-CN-PPV-1** bearing nitrile groups. This behavior is shown by the water vapor sorption isotherms in the low pressure region, which is indicative of high-water-surface interactions (Figure 4b).[19] The measured Zeta potential of **2D-COOH-PPV-1** in neutral water (-73.6 mV) is much lower than the well-known graphene oxide (-43 mV),

This article is protected by copyright. All rights reserved.

Accepted Manuscript

indicating a stable dispersion in aqueous phase. A Zeta potential of -30 mV is considered as threshold for stable dispersions in water (Figure 4c).[20] The SEM image of drop-casted **2D-COOH-PPV-1** in water shows a homogeneous polymer film formation, which further supports good solution processability of the hydrolysed polymer than the parent **2D-CN-PPV-1** (Figure S7-2, ESI).

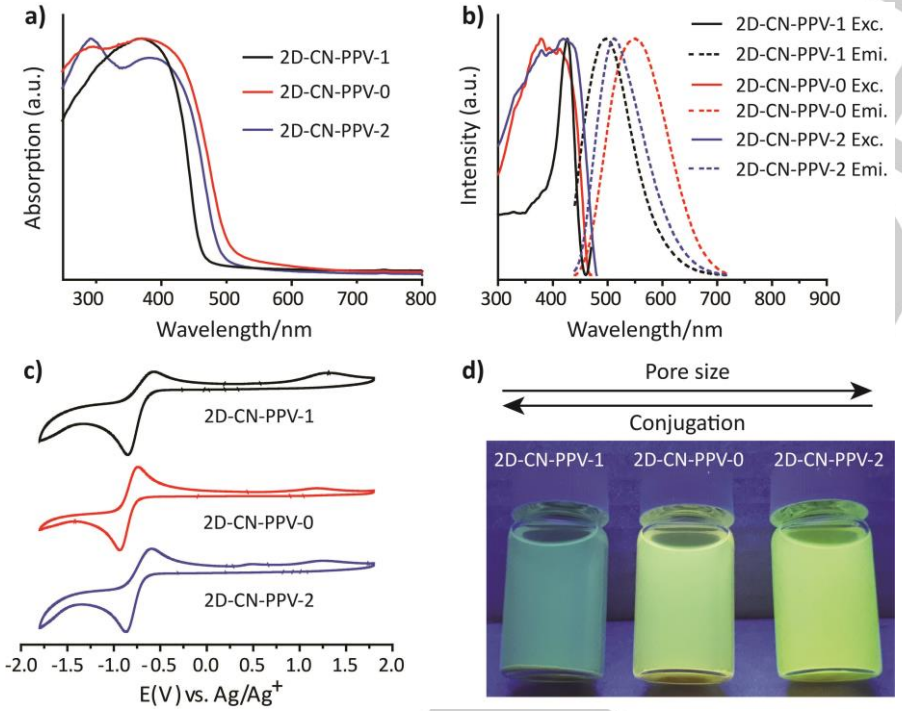

Figure 3. UV/Vis absorption and b) PL spectra (λ_{ex} = 420 nm at 25 °C) of 2D-CN-PPVs from dispersions in isopropanol; c) CV (in acetonitrile with 0.1 M $[nBu_4N][PF_6]$ as electrolyte, measured at a scan rate of 0.1 V s^{-1}) from 2D-CN-PPV-1 (black), 2D-CN-PPV-0 (red) and 2D-CN-PPV-2 (blue), respectively. d) Photo of 2D-CN-PPVs dispersed in Ethanol under 365 nm UV-light irradiation.

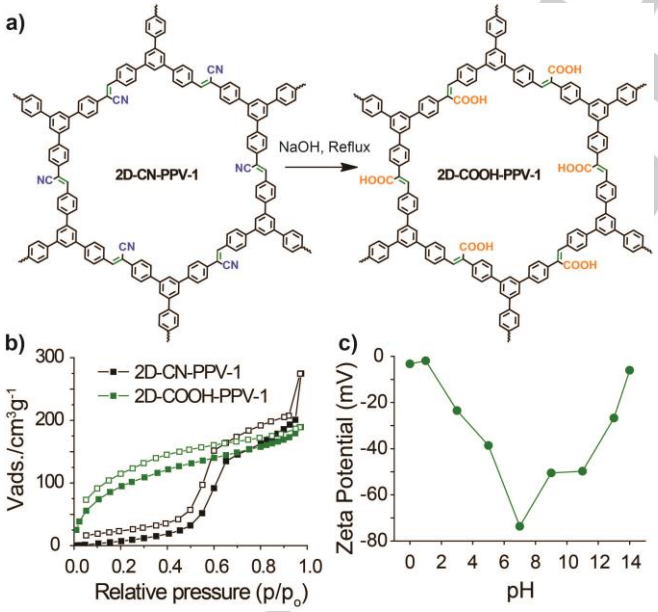

Figure 4. a) Schematic illustration of post-synthetic modification of **2D-CN-PPV-1** to **2D-COOH-PPV-1**; b) water absorption isotherms; c) Zeta Potential of **2D-COOH-PPV-1** (0.05 mg/mL) in water of **2D-COOH-PPV-1** (green) and **2D-CN-PPV-1** (black), respectively.

Remarkably enough, the hydrolyzed polymer **2D-COOH-PPV-1** well maintained its crystallinity and, thus structural integrity (Figure S4-4, ESI). Solid state UV/Vis measurements showed an absorption edge of 467 nm for **2D-COOH-PPV-1**, which is consistent to the absorption edge of 465 nm for **2D-CN-PPV-1** (Figure S5-1, ESI).

Conclusions

In summary, we demonstrate two novel 2D cyano- substituted polyphenylene vinylene polymers by controlling the Knoevenagel condensation reaction, and conduct a deep study on the crystalline 2D conjugated polymer formation as a function of inorganic Lewis bases and explore their optoelectronic properties. Our experimental and theoretical results disclose the crucial and unique role of the base in the formation mechanism for polymerizations in 2D. We propose a quantifiable energy diagram of a “quasi-reversible reaction” which allows to identify further suitable C-C bond formation reactions for new 2D conjugated polymers. Furthermore, we delineate the narrowing of the HOMO-LUMO band gaps of 2D conjugated polymers with increasing conjugation and reveal the significant cross-conjugation over *meta*-linkages. A post-modification of 2D-CN-PPVs was developed through hydrolysis, which results into high surface polarity and better solution processability from aqueous solution. We believe that our work will provide novel insight into the synthetic development of emerging crystalline 2D conjugated polymers with low band gaps for applications in organic electronics.

Accepted Manuscript

This article is protected by copyright. All rights reserved.

Conflict of Interest

There are no conflicts to declare.

Acknowledgements

This research was supported financially by the EC under Graphene Flagship (No. CNECT-ICT-604391), the Center for Advancing Electronics Dresden (cfaed), the European Union/European Social Fund and the Free State of Saxony (ESF project "GRAPHD", TU Dresden). We thank Dr. Philipp Schlender for P-XRD, Dr. Tilo Lübken for NMR in solution, M.Sc. Felix Fries and Prof. Dr. Sebastian Reineke for PLQY measurements, M.Sc. Sven Grätz and Dr. Lars Borchardt for vaporsorption measurements and Dresden Center for Nanoanalysis (DCN) and Mr. SangWook Park for SEM, Mr. Hafesudeen Sahabudeen and Mr. Kejun Liu for TEM measurements. We also acknowledge Dr. Renhao Dong, Dr. Junzhi Liu for helpful discussions and Ms. Verena Müller for practical support as student research assistant. Computational resources were provided by the Center for Information Services and High Performance Computing (ZIH) of the Technische Universität Dresden.

Keywords: 2D Conjugated Polymers • Polyphenylene Vinylene • Density Functional Calculations • Optoelectronics • Post-synthetic Modification

[1] a) "The Nobel Prize in Chemistry 2000 – Advanced Information". Nobelprize.org. Nobel Media AB 2014. Web. 9 May 2018. <http://www.nobelprize.org/nobel_prizes/chemisty/laureates/2000/advanced.html>.

[2] a) M. Mizukami, S. Cho, K. Watanabe, M. Abiko, Y. Suzuri, S. Tokito, J. Kido, *IEEE Electron. Dev. Lett.* **2018**, *1*, 39–42; b) B. Geffroy, P. le Roy, C. Prat, *Polym. Int.* **2006**, *55*, 572–582; c) J. Hou, O. Inganäs, R. H. Friend, F. Gao, Nature Mater. **2018**, *17,* 119–128; d) H. S. Vogelbaum, G. Sauvé, *Synth. Met.* **2017**, *223*, 107–121; e) C. D. Dimitrakopoulos, D. J. Mascaro, *IBM J. Res. Dev*. **2001**, *45*, 11–27; f) S. R. Forrest, M. E. Thompson, *Chem. Rev.* **2007**, *107*, 4, 923–925; g) C. L. Chochos, S. A. Choulis, *Prog. Polym. Sci*. **2011**, *36*, 1326–1414; h) A. Moliton, R. C Hiorns, *Polym. Int.* **2004**, *53*, 1397–1412; i) K. F. Wong, M. S. Skaf, C. Yang, P. J. Rossky, B. Bagchi, D. Hu, J. Yu, P. F. Barbara, *J. Phys. Chem. B* **2001**, *105*, 6103–6107.

[3] A. D. Yoffe, *Adv. Phys.* **1993**, *42*, 173–262.

[4] A. C. Ferrari, F. Bonaccorso, V. Fal'ko, K. S. Novoselov, S. Roche, P. Bøggild, S. Borini, F. H. L. Koppens, V. Palermo, N. Pugno, J. A. Garrido, R. Sordan, A. Bianco, L. Ballerini, M. Prato, E. Lidorikis, J. Kivioja, C. Marinelli, T. Ryhänen, A. Morpurgo, J. N. Coleman, V. Nicolosi, L. Colombo, A. Fert, M. Garcia-Hernandez, A. Bachtold, G. F. Schneider, F. Guinea, C. Dekker, M. Barbone, Z. Sun, C. Galiotis, A. N. Grigorenko, G. Konstantatos, A. Kis, M. Katsnelson, L. Vandersypen, A. Loiseau, V. Morandi, D. Neumaier, E. Treossi, V. Pellegrini, M. Polini, A. Tredicucci, G. M. Williams, B. Hee Hong, J.-H. Ahn, J. Min Kim, H. Zirath, B. J. van Wees, H. van der Zant, L. Occhipinti, A. Di Matteo, I. A. Kinloch, T. Seyller, E. Quesnel, X. Feng, K. Teo, N. Rupesinghe, P. Hakonen, S. R. T. Neil, Q. Tannock, T. Löfwander, J. Kinaret, *Nanoscale*, **2015**, *7*, 4598.

[5] a) R. Gutzler, D. F. Perepichka, *J. Am. Chem. Soc.* **2013**, *135*, 16585−16594; b) B. Lukose, A. Kuc, J. Frenzel, T. Heine, *Beilstein J. Nanotechnol.* **2010**, *1*, 60–70.

[6] a) M. Bieri, M. Treier, J. Cai, K. Ait-Mansour, P. Ruffieux, O. Gröning, P. Gröning, M. Kastler, R. Rieger, X. Feng, K. Müllen, R. Fasel, *Chem. Commun*. **2009**, 6919–6921; b) M. Bieri, M. Nguyen, O. Gröning, J. Cai, M. Treier, K. Ait-Mansour, P. Ruffieux, C. A. Pignedoli, D. Passerone, M. Kastler, K. Müllen, R. Fasel, *J. Am. Chem. Soc.* **2010**, *132*, 16669–16676; c) L. Grill, M. Dyer, L. Lafferentz, M. Persson, M. V. Peters, S. Hecht, *Nature Nanotech.* **2007**, *2*, 687–691; d) L. Lafferentz, V. Eberhardt, C. Dri, C. Africh, G. Comelli, F. Esch, S. Hecht, L. Grill, *Nature Chem.* **2012**, *4*, 215–220.

[7] W. Liu, X. Luo, Y. Bao, Y. P. Liu, G.-H. Ning, I. Abdelwahab, L. Li, C. T. Nai, Z. G. Hu, D. Zhao, B. Liu, S. Y. Quek, K. P. Loh, *Nature Chem.* **2017**, *9*, 563–570.

[8] a) D. B. Shinde, H. B. Aiyappa, M. Bhadra, B. P. Biswal, P. Wadge, S. Kandambeth, B. Garai, T. Kundu, S. Kurungot, R. Banerjee, *J. Mater. Chem. A* **2016**, *4*, 2682–2690; b) C. S. Diercks, O. M. Yaghi, *Science* **2017**, *355*, eaal1585; c) N. Huang, P. Wang, D. Jiang, *Nature Rev. Mater.* **2016**, *1*, 16068; d) V. S. Vyas, F. Haase, L. Stegbauer, G. Savasci, F. Podjaski, C. Ochsenfeld, B. V. Lotsch, *Nature Commun.* **2015**, *6*, 8508; e) L. Stegbauer, K. Schwinghammer, B. V. Lotsch, *Chem. Sci.* **2014**, *5*, 2789–2793; f) H. Sahabudeen, H. Qi, B. A. Glatz, D. Tranca, R. Dong, Y. Hou, T. Zhang, C. Kuttner, T. Lehnert, G. Seifert, U. Kaiser, A. Fery, Z. Zheng, X. Feng, *Nature Commun*. **2016**, *7*, 13461; g) S. Yu, J. Mahmood, H. Noh, J. Seo, S. Jung, S. Shin, Y. Im, I. Jeon, J. Baek, *Angew. Chem*. **2018**, *130*, 8574.

[9] X. Zhuang, W. Zhao, F. Zhang, Y. Cao, F. Liu, S. Bi, X. Feng, *Polym. Chem.* **2016**, *7*, 4176–4181.

[10] a) E. Jin, M. Asada, Q. Xu, S. Dalapati, M. A. Addicoat, M. A. Brady, H. Xu, T. Nakamura, T. Heine, Q. Chen, D. Jiang, *Science* **2017**, *357*, 673–676; b) S. Xu, G. Wang, B. P. Biswal, M. Addicoat, S. Paasch, W. Sheng, X. Zhuang, E. Brunner, T. Heine, R. Berger, X. Feng, *Angew. Chem. Int. Ed.* **10.1002/anie.201812685;** c) E. Jin, J. Li, K. Geng, Q. Jiang, H. Xu, Q. Xu, D. Jiang, *Nature Commun*. **2018**, *9*, 4143.

[11] a) B. P. Biswal, S. Chandra, S. Kandambeth, B. Lukose, T. Heine, R. Banerjee, *J. Am. Chem. Soc.* **2013**, *135*, 5328−5331; b) R. Dong, P. Han, H. Arora, M. Ballabio, M. Karakus, Z. Zhang, N. Chandrasekhar, P. Adler, P. St. Petkov, A. Erbe, S. C. B. Mannsfeld, C. Felser, T. Heine, M. Bonn, X. Feng, E. Cánovas, *Nature Materials* **2018**, *17*, 1027; c) R. Dong, Z. Zhang, D. Tranca, S. Zhou, M. Wang, P. Adler, Z. Liao, F. Liu, Y. Sun, W. Shi, Z. Zhang, E. Zschech, S. C. B. Mannsfeld, C. Felser, X. Feng, *Nature Commun*. **2018**, *9*, 2637.

[12] a) Cesium cation with 167 pm in diameter is the biggest cation. Other sizes: Rb^+: 152 pm, K^+: 138 pm, Na^+: 102 pm, Ba^{2+}: 135 pm; b) R. D. Shannon, C. T. Prewitt, *Acta Cryst. B* **1969**, *25*, 925–946; c) R. D. Shannon, *Acta Cryst. A* **1976**, *32*, 751–767.

[13] C. M. Thompson, G. Occhialini, G. T. McCandless, S. B. Alahakoon, V. Cameron, S. O. Nielsen, R. A. Smaldone, *J. Am. Chem. Soc.* **2017**, *139*, 10506–10513.

[14] K. S. W. Sing, *Pure Appl.Chem.* **1982**, *54*, 2201—2218.

[15] https://www.perkinelmer.com/lab-solutions/resources/docs/APP_UVVISNIRMeasureBandGapEnergyValue.pdf; Web. 20 September 2018.

[16] M. Hanack, B. Behnisch, H. Hackl, P. Martinez-Ruiz, K.-H. Schweikart, *Thin Solid Films*, **2002**, *417*, 26–31.

[17] a) M. Helbig, H.-H. Hörhold, *Makromol. Chem*. **1993**, *194*, 1607-1618; b) H.-H. Hörhold, *Z. Chem*. **1972**, *12*, 41-52; c) H. Tillmann. H.-H. Hörhold, *Synthetic Metals*, **1999**, *101*, 138-139; d) S. V. Chasteen, S. A. Carter, G. Rumbles, *J. Chem. Phys*. **2006**, *124*, 214704; e) T. Wu, R. Sheu, Y. Chen, *Macromolecules* **2004**, *37*, 725-733.

[18] a) S. C. Moratti, R. Cervini, A.B. Holmes, D. R. Baigent, R. H. Friend, N.C. Greenham, J. Grüner, and P. J. Hamer, *Synthetic Metals*, **1995**, *71*, 2117-2120; b) C. Chang, C Wang, C. Chao, M. Lin, *J. Polym. Res*. **2005**, *12*, 1; c) T. Ahn, M. S. Jang, H. Shim, D. Hwang, T. Zyung, *Macromolecules* **1999**, *32*, 3279; d) N. C. Greenham, R. H. Friend, D. Bradley, *Adv. Mater*. **1994**, *6*, 6.

[19] a) E. Zhang, G.-P. Hao, M. E. Casco, V. Bon, S. Grätz, L. Borchardt, *J. Mater. Chem. A*, **2018**, *6*, 859–865; b) T. Horikawa, N. Sakao, T. Sekida, J. Hayashi, D.D. Do, M. Katoh, *Carbon*, **2012**, *50*, 1833-1842; c) L. F. Velasco, D. Snoeck, A. Mignonm L. Misseeuw, C. O. Ania, S. Van Vlierberghe, P. Dubruel, N. de Belie, P. Lodewyckx, *Carbon*, **2016**, *106*, 284-288, d) K. Kaneko, Y. Hanzawa, T. Iiyama, T. Kanda and T. Suzuki, *Adsorption*, **1999**, *5*, 7–13; e) P.-X. Hou, H. Orikasa, T. Yamazaki, K. Matsuoka, A. Tomita, N. Setoyama, Y. Fukushima, T. Kyotani, *Chem. Mater*. **2005**, *17*, 5187-5193

[20] a) D. Li, M. B. Müller, S. Gilje, R. B. Kaner, G. G. Wallace, *Nat. Nanotech.* **2008**, *3*, 101; b) Everett, D. H. *Basic Principles of Colloid Science* (The Royal Society of Chemistry, London, **1988**).

Accepted Manuscript

This article is protected by copyright. All rights reserved.

10.1002/chem.201806385

WILEY-VCH

FULL PAPER

In this work, we present the efficent synthesis of two novel 2D fully sp²-carbon-linked crystalline PPVs and investigate the essentiality of inorganic bases for their catalytic formation. Notably, among all bases screened, cesium carbonate (Cs_2CO_3) plays a crucial role and enables reversibility in the first step with subsequent structure locking by formation of a C=C double bond to maintain crystallinity, which is supported by density functional theory (DFT) calculation.

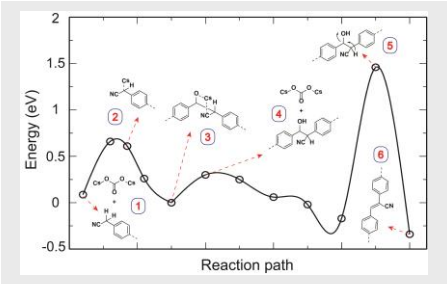

Daniel Becker, Bishnu P. Biswal, Paula Kaleńczuk, Naisa Chandrasekhar, Lars Giebeler, Matthew Addicoat, Silvia Paasch, Eike Brunner, Karl Leo, Arezoo Dianat, Gianaurelio Cuniberti, Reinhard Berger, Xinliang Feng**

Page No. 1 – Page No. 7

Title

Fully sp²-Carbon-Linked Crystalline Two-Dimensional Conjugated Polymers: Insight into 2D Poly(Phenylenecyanovinylene) Formation and Their Optoelectronic Properties

WILEY-VCH
Accepted Manuscript

This article is protected by copyright. All rights reserved.